

Formation dynamics of hexadecanethiol self-assembled monolayers on (001) GaAs observed with photoluminescence and Fourier transform infrared spectroscopies

Chan-Kyu Kim,¹ Gregory M. Marshall,^{1,2} Matthieu Martin,¹ Michel Bisson-Viens,¹ Zbigniew Wasilewski,³ and Jan J. Dubowski^{1,a)}

¹Department of Electrical and Computer Engineering, Université de Sherbrooke, Sherbrooke, Québec J1K 2R1, Canada

²Institute for Chemical Process and Environmental Technology, National Research Council of Canada, Ottawa, Ontario K1A 0R6, Canada

³Institute for Microstructural Sciences, National Research Council of Canada, Ottawa, Ontario K1A 0R6, Canada

(Received 31 May 2009; accepted 21 September 2009; published online 26 October 2009)

The dynamics of hexadecanethiol (HDT) [HS(CH₂)₁₅CH₃] chemisorption and the formation of a self-assembled monolayer (SAM) on the GaAs(001) surface was studied *in situ* by monitoring the photoluminescence (PL) intensity over a 20 h period. Comparing the PL time series in HDT solution with that of the bare GaAs surface similarly exposed to the ethanol solvent, we observed a two-phased evolution of the associated PL enhancement. Time-commensurate changes in the absorption frequency and intensity of the C–H stretching mode vibrations were then recorded using Fourier transform infrared spectroscopy, supporting that the PL enhancement corresponds directly with known mechanisms of ordered SAM formation. These results highlight the sensitivity with which *in situ* PL monitoring can reflect surface processes and underscores its potential for use in sensor applications. © 2009 American Institute of Physics. [doi:10.1063/1.3248370]

I. INTRODUCTION

Sensing based on the analysis of surface phenomena is an attractive approach for the detection and identification of biomolecules and chemical species, with the potential to advance molecular diagnostics and other biomedical applications.^{1–8} For metal surfaces such as Au, the fundamental interface applied in numerous biosensing architectures is based on the monolayer chemisorption and self-assembly of various thiol group (R-SH) molecules.^{7–9} The formation of self-assembled monolayers (SAMs) using long-chain alkanethiols on the GaAs(001) surface has been studied by several authors,^{10–21} and is of growing interest in the biosensing domain. This interest is in part due to the surface passivation effect demonstrated by covalent thiol bonding,^{11,14,17,18,22} and in part due to the ability of the SAM to immobilize various analyte binding systems through a functional endgroup, DNA, or other biomolecular couplings including biotin.^{2,23}

GaAs is an attractive design candidate for a surface-based device because of its unique chemical, electrical, and optical properties that can be directly controlled by surface modification.^{17,24,25} With a surface density of states exceeding 10^{12} cm⁻² eV⁻¹,²⁶ the GaAs(001) surface nominally retains a significant number of midgap trapped charges resulting in surface Fermi level pinning.²⁷ The passivation of nonradiative centers effected by the chemisorption of sulfur derived species results in a decrease in surface recombination velocity with a corresponding enhancement in photolumines-

cence (PL) intensity, as found by Lunt *et al.*¹¹ A correlation of PL with the electron donating ability of the passivating agent was also reported,¹¹ suggesting that an electrostatic phenomenon is associated with the surface state. Modulation of the PL through mediation of the electronic parameters offers a means of transduction in a sensor platform, consequently, as it is expected that chemical reactions or the presence of molecular fields can affect changes in the local surface potential. The precise nature of this mechanism is an actively pursued area of our group's research.

In order to study the effects of surface modification in the context of sensor development, *in situ* PL measurements are desirable owing to the relative nature of the measurement and their ability to monitor time-dependent phenomena. With this in mind, we present for the first time a continuous *in situ* measurement of PL intensity during the process of hexadecanethiol (HDT) [HS(CH₂)₁₅CH₃] SAM formation on GaAs(001), illustrating the surface molecular dynamics in quasi-real-time. The evolution of SAM coverage and molecular order is also characterized by Fourier transform infrared (FTIR) spectroscopy as a prototypical example, and is correlated with our PL results in an effort to demonstrate the sensitivity of PL surface modification to surface dynamic processes.

II. EXPERIMENTAL DETAILS

PL measurements were carried out using a custom-designed hyperspectral imaging PL mapper (HI-PLM) that accommodates samples up to 7×7 mm² providing a spatial resolution of 5 μm approximately. The full sample area is excited with a continuous wave 532 nm laser in this system,

^{a)}Tel.: (819) 821–8000. FAX: (819) 821–7937. Electronic mail: jan.j.dubowski@usherbrooke.ca.

and mapping acquisition in the spectral region of interest takes about 70 s typically. In our study, the computer-based interface of the HI-PLM system automated the collection of a time series of PL maps in 10 min intervals. Sample illumination was controlled by a computer-programmed shutter that opened during PL integration time only. Dark maps were also recorded and used for background subtraction. A fused silica window reflected 4% of the excitation source to a Centronic OSD100-7Q calibrated silicon photodiode for power normalization, establishing PL stability within 3% variation. The PL spectrum peak intensity derived from each map represents the spatial average, in this case for uniform samples.

A nominally undoped GaAs/AlGaAs multilayer structure grown by molecular beam epitaxy on a semi-insulating (001) GaAs substrate was employed for the deposition of the investigated HDT-SAM. The structure is comprised of a 100 nm GaAs layer on which a $20\times$ (2.4 nm GaAs/2.4 nm AlAs) superlattice was grown. This was followed by a 300-nm-thick GaAs buffer layer overlaid with 100 and 5-nm-thick $\text{Al}_{0.33}\text{Ga}_{0.67}\text{As}$ films confining a 6-nm-thick GaAs quantum well. The microstructure was capped with a 5-nm-thick GaAs layer. Strong room temperature PL at 870 nm was observed from the buffer layer only. By virtue of the carrier-confining properties of the superlattice, diffusion from the buffer layer was made less efficient resulting in excess carrier density in the surface region and increased PL yield. The brightness of the imaging system was improved consequently, compensating for the low excitation power density ($<500\text{ mW/cm}^2$) employed as a result of the use of flood illumination. Some trade-off in surface sensitivity for image brightness is implicit in this discussion.

The details of HDT-SAM preparation and the recording of FTIR spectra are reported elsewhere.¹⁹ For the latter, semi-insulating GaAs material was used in order to accommodate transmission measurements with low signal attenuation. IR spectra were recorded *ex situ* after a variable period of SAM incubation. For the PL measurements, samples were monitored continuously in HDT solution, sealed in a Teflon cell with a fused silica window for direct *in situ* measurement. For PL referencing, a freshly etched but untreated GaAs sample was monitored under the same conditions.

III. RESULTS AND DISCUSSION

A. Effect of excitation power density on PL intensity

The PL signal intensity from GaAs depends not only on the surface quality and surface coverage of chemisorbed thiols, but also on the power density of the excitation light source. Figure 1 shows the dependence of PL intensity on laser power density under equivalent conditions of HDT-SAM formation. Degradation of the PL is clear from the trace in Fig. 1(a) using 463 mW/cm^2 . As the power density is reduced to 146 and 113 mW/cm^2 , photodegradation is suppressed as shown in Figs. 1(b) and 1(c), respectively. At the lowest density, the surface dynamics of SAM formation become clear and appear to trend toward saturation levels. Note that in other reported work, the suppression of PL photodegradation in sulphide treated GaAs was achieved using a power density of 2 W/cm^2 in a nonstructured wafer.²⁴ In

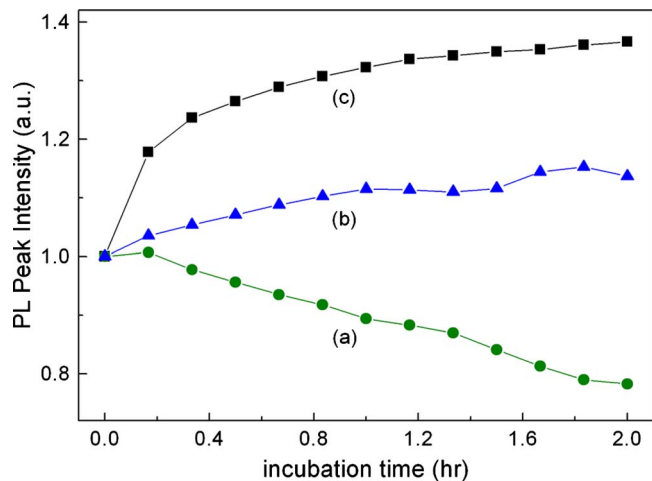


FIG. 1. (Color online) Reduction in the photodegradation effect observed during HDT-SAM incubation. Applied laser power density: (a) 463 , (b) 146 , and (c) 113 mW/cm^2 . Values are normalized to the initial condition.

this case, under focused beam conditions and a direct path for diffusion to the bulk, the accumulation of surface charge that may persist and retard radiative recombination is minimized. In contrast, the broad area illumination, the use of a confinement structure and long integration times in our experiment are the likely reasons why 20 times less power density was required to avoid the degradation effect.

B. Dynamics of thiolation observed by PL

Figure 2(a) shows the evolution of PL emitted from the GaAs buffer during the HDT-SAM formation process over a 20 h period. In terms of the surface dynamics, we expect that thiol molecules will first physisorb uniformly on the GaAs capping layer, chemisorbing to either Ga or As surface atoms.^{16,28} The highly covalent nature of bonding allows electron sharing with the surface as cited above, increasing the PL efficiency by reducing the recombination velocity from the buffer layer to the surface. Similar enhancement effects due to a reduction in the surface diffusion rate across

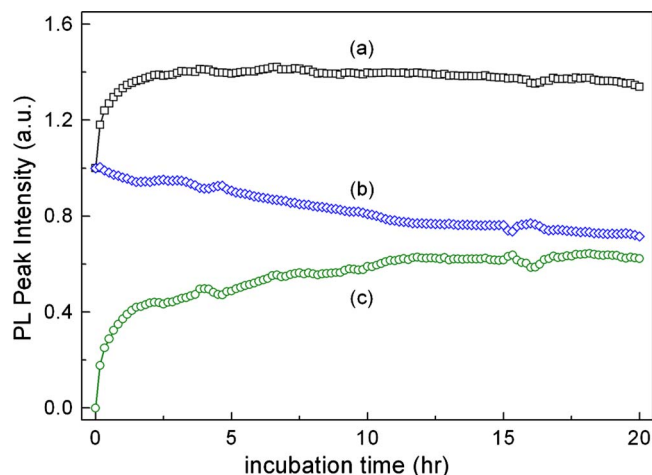


FIG. 2. (Color online) Evolution of the PL peak intensity from the etched GaAs structure exposed to (a) 2 mM of HDT dissolved in degassed ethanol and (b) degassed ethanol. Values are normalized to the initial condition. The differential PL intensity in (a) and (b) is shown in (c).

an AlGaAs barrier from buried InAs quantum dots have been observed following alkanethiol treatment of a GaAs capping layer.²⁹ By analogy, we expect our results to be dominated by similar transport mechanisms, since the scale of enhancement is about the same (1.6 times) in our data. Carrier pairs are generated in our structure within a few optical penetration depths (<300 nm), which does not exceed the diffusion length for GaAs, and recall that carriers are confined from transport into the depth of the substrate by the AlAs/GaAs superlattice. Therefore, it is plausible that the PL from the buffer layer can be directly affected by surface adsorption by virtue of the surface recombination current. Once sufficient surface coverage is achieved, the HDT molecules will begin close-packing by van der Waals attraction. Also, hydrogen obtained by the cleavage of S–H bonds may remain on the surface and play an important role in the kinetics of adsorption and desorption.¹⁶ These complex chemisorption and SAM formation processes determine the rate of surface coverage and therefore the dynamic rate of PL increase.

PL intensity from the reference structure, with etched GaAs cap exposed to ethanol solution only, is shown in Fig. 2(b) demonstrating a significant decrease in PL intensity from the onset. Since degassed ethanol was used in this experiment, we rule out that surface reoxidation would be a major factor contributing to the observed PL decay. An alternative process could be related to the modification of the surface electric dipole by the solvation of ethanol molecules around active defect sites on the GaAs surface. This description follows in a manner similar to that forwarded by Bessolov *et al.*,³⁰ where solvation about the ionic character of sulphide-GaAs bonds was thought to affect the near-surface electronic state. We expect that close-packing in the SAM would exclude solvation effects around the thiol-GaAs bond, but defect site modification may still be plausible for the SAM, e.g., around domain boundaries or various inclusions.

The data series in Figs. 2(a) and 2(b) were subtracted to yield the differential PL intensity as shown in Fig. 2(c), exclusive of defect modification effects. The maximum differential PL enhancement is about 1.6 times higher than the PL signal initially and the evolution suggests a two-stage kinetic process, as discussed further below, in qualitative agreement with a model suggested by McGuinness *et al.*¹⁴

C. Dynamics of HDT thiolation observed by FTIR

The results of FTIR spectroscopy are reported in Fig. 3, showing the peak absorption intensities [Fig. 3(a)] and vibrational energies [Fig. 3(b)] of the asymmetric C–H stretching mode (ν_{as}) of alkane CH₂. The inset shows the spectrum recorded after 22 h incubation and represents the stabilized formation. Highlighted are the characteristic C–H vibrational energies of the symmetric (ν_s) and asymmetric stretching modes of CH₂, and the asymmetric stretching modes of CH₃ (ν_{a3}). In our results, ν_{as} shows a clear trend toward saturation levels, both in terms of increasing peak intensity and decreasing peak frequency. The IR parameters relate to the evolution of SAM formation according to known mechanisms. These include a rapid adsorption phase, followed by a slow reaction where the surface density continues to increase and

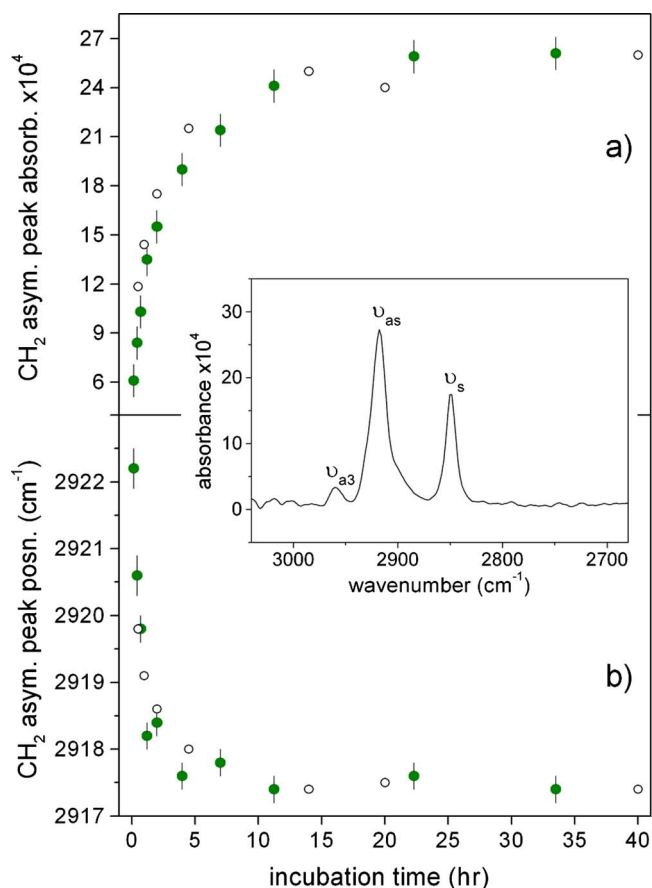


FIG. 3. (Color online) (a) FTIR peak absorbance and (b) position of the asymmetric (ν_{as}) C–H stretching mode of alkane CH₂ in HDT-SAMs. Closed/open points represent separate data series. Error bars are estimated from baseline uncertainty. Inset: IR spectrum after stabilized formation (22 h) illustrating the asymmetric and symmetric (ν_s) C–H stretching modes, and the asymmetric stretching modes of CH₃ (ν_{a3}).

the conformational disorder of the alkane is reduced.¹⁴ In addition, the effects of molecular orientation and extrinsic surface enhancement phenomena act to increase the IR absorbance.

D. Comparison between PL and FTIR measurement

In order to quantify the dynamics of HDT-SAM formation, the evolution of PL and IR signals were normalized to their respective saturation peak intensities and fitted with a generalized two-term exponential function according to

$$I = 1 - A_1 e^{-t/\tau_1} - A_2 e^{-t/\tau_2}, \quad (1)$$

where the coefficients are subject to $A_1 + A_2 = 1$ in order to conform to the boundary conditions at $t = 0$. Normalization was based on the saturation implicit in the Langmuir adsorption model.^{31,32}

Fitting of the normalized differential PL intensity (I_{PL}) according to Eq. (1) yielded the following result and is plotted in Fig. 4

$$I_{PL} = 1 - 0.52 e^{-t/0.28} - 0.48 e^{-t/6.2}. \quad (2)$$

From this empirical result, we observe there are two mechanisms responsible for the dynamic adsorption rate. The first exponential term ($t_1 = 0.28$ hr) corresponds to the rapid pro-

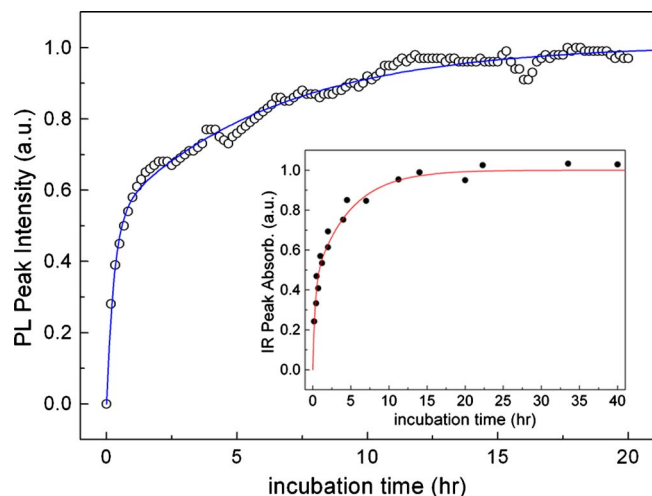


FIG. 4. (Color online) Peak PL intensity and IR absorbance with fitting results corresponding to Eqs. (2) and (3). Data are normalized to the respective saturation values of each curve.

cess of thiol-surface interaction, which dominates at times < 1 h. The second term reflects a secondary process with a much longer time constant ($t_2 = 6.2$ h), i.e., the molecular ordering phase as expected. The large difference in time constants suggests the second process is distinct, becoming significant only as the first one approaches saturation. The double exponential behavior of the observed surface dynamics indicates that *in situ* PL is an effective technique, sensitive not only to chemisorption binding events, but also to the rate at which these occur, which is governed by two discernable process characteristics.

Shown in the inset of Fig. 4, the time dependence of the normalized IR intensity (I_{IR}) agrees with the form of the PL time profile and is similarly fitted according to Eq. (1),

$$I_{\text{IR}} = 1 - 0.43e^{-t/0.30} - 0.57e^{-t/4.6}, \quad (3)$$

verifying the two process rates as observed in Eq. (2). The scaling of the shorter time constant appears about two times less than has been reported previously,¹⁴ but more importantly, it is equivalent to that observed in the PL data. This equivalence suggests the IR and PL dynamics are dominated by the same rapid absorption rate in the initial phase. However, as described in the previous section, there are additional factors responsible for IR absorbance not expected to affect the PL directly, i.e., processes that do not affect the surface adsorption rate. These factors would be expected to blur the IR response with respect to the surface adsorption dynamics manifesting only once the conformational order in the SAM started to increase. The smaller value of the time constant in the second term of Eq. (3) relative to Eq. (2) suggests this may be a valid interpretation, i.e., convolution by these additional factors results in less demarcation between the surface adsorption dynamics and molecular ordering dynamics observed in IR. In this manner, *in situ* PL has shown itself more capable of resolving the dynamic surface adsorption rate, and by way of our example, demonstrates the sensitivity with which surface adsorption and molecular ordering processes may be monitored by this technique.

IV. CONCLUSIONS

The formation dynamics of HDT-SAMs on GaAs were observed by monitoring the PL signal *in situ* and by recording the IR absorption over time with a view to the recognition of distinct surface dynamic processes. A two-term exponential time-dependent increase in the PL intensity was found, indicating two contributing factors to the dynamic adsorption and molecular organization rates, with 0.28 and 6.2 h time constants, respectively. Commensurate with the PL data, time-dependent observations of the IR intensity and vibrational frequency were also made. These demonstrated a two-phase surface dynamic as expected, but with less differentiated time constants, indicating convoluting factors not reflected in the PL data. From these results, we have demonstrated that *in situ* PL offers a highly sensitive technique for monitoring dynamic surface adsorption and molecular organization processes.

ACKNOWLEDGMENTS

Funding for this research was provided by the Natural Sciences and Engineering Research Council of Canada (Grant No. STPGP 350501-07), the Canada Research Chair in Quantum Semiconductors Program (J.J.D.) and the National Research Council of Canada Graduate Student Scholarship Supplement Program (G.M.M.).

- ¹J. J. Dubowski, in *Photon-Based Nanoscience and Nanobiotechnology*, edited by J. J. Dubowski and S. Tanev (Springer, Netherlands, 2006), Vol. 236, p. 159.
- ²X. Ding, Kh. Moumanis, J. J. Dubowski, E. H. Frost, and E. Escher, *Appl. Phys. A: Mater. Sci. Process.* **83**, 357 (2006).
- ³R. R. Kale, H. Mukundan, D. N. Price, J. F. Harris, D. M. Lewallen, B. I. Swanson, J. G. Schmidt, and S. S. Iyer, *J. Am. Chem. Soc.* **130**, 8169 (2008).
- ⁴X. D. Hoa, A. G. Kirk, and M. Tabrizian, *Biosens. Bioelectron.* **23**, 151 (2007).
- ⁵L. Nicu and T. Leïchl , *J. Appl. Phys.* **104**, 111101 (2008).
- ⁶C. K. Kim, R. R. Kalluru, J. P. Singh, A. Fortner, J. Griffin, G. K. Darbha, and P. C. Ray, *Nanotechnology* **17**, 3085 (2006).
- ⁷Z. Zhao, I. Banerjee, and H. Matsui, *J. Am. Chem. Soc.* **127**, 8930 (2005).
- ⁸K. L. Brogan and M. H. Schoenfish, *Langmuir* **21**, 3054 (2005).
- ⁹D. Peelen and L. M. Smith, *Langmuir* **21**, 266 (2005).
- ¹⁰O. S. Nakagawa, S. Ashok, S. W. Sheen, J. Martensson, and D. L. Allara, *Jpn. J. Appl. Phys., Part 1* **30**, 3759 (1991).
- ¹¹S. R. Lunt, G. N. Ryba, P. G. Santangelo, and N. S. Lewis, *J. Appl. Phys.* **70**, 7449 (1991).
- ¹²J. F. Dorsten, J. E. Maslar, and P. W. Bohn, *Appl. Phys. Lett.* **66**, 1755 (1995).
- ¹³T. Baum, S. Ye, and K. Uosaki, *Langmuir* **15**, 8577 (1999).
- ¹⁴C. L. McGuinness, A. Shaporenko, C. K. Mars, S. Uppili, M. Zharnikov, and D. L. Allara, *J. Am. Chem. Soc.* **128**, 5231 (2006).
- ¹⁵Y. Jun, X. Y. Zhu, and J. W. P. Hsu, *Langmuir* **22**, 3627 (2006).
- ¹⁶O. Voznyy and J. J. Dubowski, *J. Phys. Chem. B* **110**, 23619 (2006).
- ¹⁷X. Ding, Kh. Moumanis, J. J. Dubowski, L. Tay, and N. L. Rowell, *J. Appl. Phys.* **99**, 054701 (2006).
- ¹⁸Kh. Moumanis, X. Ding, J. J. Dubowski, and E. H. Frost, *J. Appl. Phys.* **100**, 034702 (2006).
- ¹⁹G. M. Marshall, F. Bensebaa, and J. J. Dubowski, *J. Appl. Phys.* **105**, 094310 (2009).
- ²⁰O. Voznyy and J. J. Dubowski, *J. Phys. Chem.* **112**, 3726 (2008).
- ²¹O. Voznyy and J. J. Dubowski, *Langmuir* **24**, 13299 (2008).
- ²²T. Hou, C. M. Greenlief, S. W. Keller, L. Nelen, and J. F. Kauffman, *Chem. Mater.* **9**, 3181 (1997).
- ²³L. Mohaddes-Ardabili, L. J. Mart nez-Miranda, J. Silverman, A. Christou, L. G. Salamanca-Riba, and M. Al-Sheikhly, *Appl. Phys. Lett.* **83**, 192 (2003).

- ²⁴C. Sheng Liu and J. F. Kauffman, *Appl. Phys. Lett.* **66**, 3504 (1995).
- ²⁵V. N. Bessolov, M. V. Lebedev, A. F. Ivankov, W. Bauhofer, and D. R. T. Zahn, *Appl. Surf. Sci.* **133**, 17 (1998).
- ²⁶A. Zangwill, *Physics at Surfaces* (Cambridge University Press, New York, 1998), p. 102.
- ²⁷W. E. Spicer, I. Lindau, P. Skeath, C. Y. Su, and P. Chye, *Phys. Rev. Lett.* **44**, 420 (1980).
- ²⁸C. L. McGuinness, A. Shaporenko, M. Zharnikov, A. V. Walker, and D. L. Allara, *J. Phys. Chem. C* **111**, 4226 (2007).
- ²⁹K. Adlkofer, E. F. Duijs, F. Findeis, M. Bichler, A. Zrenner, E. Sackmann, G. Abstreiter, and M. Tanaka, *Phys. Chem. Chem. Phys.* **4**, 785 (2002).
- ³⁰V. N. Bessolov, E. V. Konenkova, and M. V. Lebedev, *J. Vac. Sci. Technol.* **14**, 2761 (1996).
- ³¹S. H. Chen and C. W. Frank, *Langmuir* **5**, 978 (1989).
- ³²A. Vilan, R. Ussyshkin, K. Gartsman, D. Cahen, R. Naaman, and A. Shanzer, *J. Phys. Chem. B* **102**, 3307 (1998).